Proceedings of the 28th IEEE
EMBS Annual International Conference
New York City, USA, Aug 30-Sept 3, 2006

Application of Velocity Filters to Somatosensory Evoked Potential Measurements for Removal of Stimulus Artifact

Nabil Yazdani, *Student Member, IEEE* Adrian D. C. Chan *Senior Member, IEEE*
Department of Systems and Computer Engineering, Carleton University, Ottawa, CANADA

***Abstract*— In this paper, velocity filtering is applied to somatosensory evoked potential (SEP) measurements to remove the stimulus artifact (SA). Using an array of electrodes, velocity information is used as a criterion for discerning the SEP from the SA. The SEP is known to propagate at speeds below 100 m/s due to nerve physiology, whereas the SA propagation mode is electromagnetic, and propagates near the speed of light. The velocity filtering method is presented, with spatial frequency resolution, physical array implementation, filter realization, and trace-to-trace consistency of the measurements identified as factors that influence overall performance. SEP data from the median nerve were recorded using an 11 channel array at the wrist, with stimulation at the index finger. These data are used to assess the velocity filtering method. The filter output is analyzed qualitatively showing a visual improvement in the SEP measurement when compared against the filter input. It is concluded that the SNR gain of the filter is promising, but distortion in the SEP estimate may occur due to spatial frequency resolution and trace-to-trace inconsistencies in the measurements.**

I. Introduction

SOMATOSENSORY evoked potentials (SEP) are bioelectric signals that propagate through nerve fibers in response to external stimuli. SEPs are useful for diagnosing neuromuscular disorders and monitoring the integrity of the nervous system [1], [2]. In noninvasive measurements, stimulation electrodes are placed on the skin surface and a large, short duration electrical pulse is used to elicit a nerve response. The SEP can be measured at a location down the nerve axon, using surface electrodes. A problem that arises is an electrical potential associated with the stimulus that appears at the measurement site. This potential is called the stimulus artifact (SA) and corrupts the SEP measurement. The SA is typically several orders of magnitude larger than the SEP, overlapping in both the time and frequency domains.

Uncorrelated noise is effectively reduced by ensemble averaging, but removal of the coherent SA requires more sophisticated methods in measurement configurations where the SEP and SA overlap. Early work approached this problem through improvements in the measurement setup and instrumentation [1], [2]. While this can help reduce the SA, a large, coherent artifact remains. Signal processing methods have been proposed as a post-processing step to remove the SA. These methods employ adaptive filters or neural networks to estimate the SA waveform and subtract it from the actual measurement [1], [3], [4]. They suffer from the fact that the estimated waveforms may differ significantly across subjects. This means a new adaptive structure must be defined and trained each time, requiring both human judgment and some element of trial and error. A velocity filtering method has recently been proposed to remove the SA [5]. This method exploits the difference in the propagation velocities of the SA and SEP. Multi-channel SEP records are obtained from a linear electrode array, and a two-dimensional FIR fan filter is directly applied to the data, which attenuates high-velocity signals and passes low-velocity signals.

Velocity filtering for SA reduction has been shown through simulation by the authors in [5], however, the SA and SEP waveforms used were simulated, with assumptions that the SA waveform was identical at every array location and the tissue filtering effect on the SEP waveform consists only of a constant time delay (i.e., constant fiber depth).

In this paper, we wish to address some of the practical issues involved with the application of velocity filters to real measurements. Section II provides an overview of velocity filters. Section III provides an explanation of the experimental procedure used. Section IV examines some factors that affect the system performance. Section V gives results and discussion of applying the velocity filter to an array of SEP measurements from the median nerve. Section VI presents some conclusions drawn from this work.

II. Velocity Filtering

Array data are expressed in one temporal and at least one spatial dimension. The signal may then be decomposed into its 2D spatio-temporal frequency spectrum using a 2D-FT given by:

$$S(k,\omega)=\int_{-\infty}^{\infty}\int_{-\infty}^{\infty}s(x,t)e^{-j\omega t}e^{-jkx}dtdx \qquad (1)$$

where t, x, ω, and k denote time, space, temporal frequency, and spatial frequency (wavenumber), respectively. The apparent velocity of a component of $s(x,t)$ at position x and time t, is transformed from the $[x,t]$ domain to the $[k,\omega]$ domain via:

$$v_{s(x,t)}=\frac{\partial x}{\partial t}\xleftarrow[\left\{\partial\omega=\frac{1}{2\pi\partial t},\partial k=\frac{1}{2\pi\partial x}\right\}]{2D-FT}\frac{\partial\omega}{\partial k}=v_{s(k,\omega)} \qquad (2)$$

Separation of signals with different velocities is accomplished by designing a 2D filter that preserves events

with velocity below a threshold (v_C) and attenuates events with velocity above this threshold. Such a filter is expressed as:

$$H(k,\omega)=\begin{cases} 1, & \left|\frac{\omega}{k}\right| < v_C \\ 0, & \text{otherwise} \end{cases} \tag{3}$$

If it is assumed that the SEP measured along the array conserves its shape across space with constant velocity, then

$$s(x,t)=s\left(t-\frac{x}{v}\right) \tag{4}$$

$$\begin{aligned} S(k,\omega) &= \int_{-\infty}^{\infty}\int_{-\infty}^{\infty} s\left(t-\frac{x}{v}\right)e^{-j\omega t}e^{-jkx}dtdx \\ &= \int_{-\infty}^{\infty} e^{\frac{-j\omega x}{v}}\left(\int_{-\infty}^{\infty} s(t)e^{-j\omega t}dt\right)e^{-jkx}dx \\ &= S(\omega)\int_{-\infty}^{\infty} e^{\frac{-j\omega x}{v}}e^{-jkx}dx \\ &= S(\omega)\delta\left(k+\frac{\omega}{v}\right) \end{aligned} \tag{5}$$

If it is further assumed that the SA conserves its shape across space with infinite velocity, then:

$$sa(x,t)=sa(t) \tag{6}$$

$$\begin{aligned} SA(k,\omega) &= \int_{-\infty}^{\infty}\int_{-\infty}^{\infty} sa(t)e^{-j\omega t}e^{-jkx}dtdx \\ &= \int_{-\infty}^{\infty}\left(\int_{-\infty}^{\infty} s(t)e^{-j\omega t}dt\right)e^{-jkx}dx \\ &= SA(\omega)\delta(k) \end{aligned} \tag{7}$$

Fig.1 shows a top view of the SEP and SA projected onto the [k,ω] plane as indicated by (3), (5), and (7). The velocity passband is the slice bounded by the radial lines representing the cutoff velocity. Ideally, the SEP is passed undistorted and the SA is rejected.

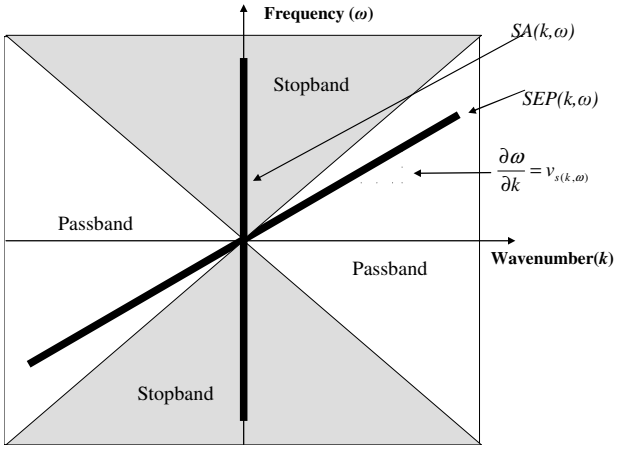

Fig.1 SA and SEP projection in [k,ω]-space

In [5], a percent-residual-difference (PRD) of 17.6% was obtained in the region containing the SEP using simulated signals under the assumptions of (4) and (6).

III. Experimental Procedure

Data were collected from a single subject (male, age 24) to assess the feasibility of velocity filtering to remove the SA from SEP measurements. In addition, we can determine and investigate the important factors that affect this method. This research was reviewed and approved by the Carleton University Research Ethics Committee.

A. Stimulation

The median nerve of the right arm was stimulated at the index finger using a Grass S48 stimulator, with a Grass SIU5 constant-voltage isolation unit. The SIU5 unit was chosen to provide good isolation, however a constant current device may produce measurements that are more repeatable by automatically tracking the required voltage to account for time-varying stimulation electrode impedance. Biphasic pulses with duration of 0.2 ms were delivered at a rate of 5 per second with amplitude of approximately 6V.

Grass F-E10S2B bipolar electrodes were used. These electrodes have twisted pair leads, 30 mm spacing, and were used with MyoTronics Myo-Jel electrolyte paste. They were placed on the index finger (palm side) along the nerve axis with the positive electrode at the distal end of the finger.

B. SEP Recording

The SEP associated with the median nerve was recorded at the wrist, using a Grass 15A54 Amplifier. The gain of the amplifier was 5000, with a bandwidth of 1 Hz to 6 kHz. A 12-bit National Instruments PCI-6071E data acquisition board (DAQ) was used to sample the measurements. Data were first collected with a sampling rate of 200 kHz and then decimated to 50 kHz in a voltage range of ±5 V.

A separate trigger pulse synchronous with each stimulus pulse was directly sent from the stimulator to the DAQ to indicate the starting time of each record. For each SEP trace, 500 triggered records were collected and ensemble averaged to reduce uncorrelated noise (e.g., electronic, cardiac, power-line, myoelectric). A 1 ms pre-trigger duration is shown in these measurements in Figure 3 for visual convenience.

Myo-Tronics Duo-Trode disposable Ag-AgCl electrodes were used to record the SEP. These contain a pair of bipolar electrodes with a fixed spacing of 20 mm. The reference electrode was a Grass F-E10SG2 silver impregnated conductive Velcro strap wrapped around the hand midway between the stimulus site and the site of the first recording channel.

The array recording of 11 channels along the median nerve axis was implemented manually by collecting each trace individually using the same electrode pair. The midpoint of the recording electrode pair for the first trace was located on the lower wrist 18.5 cm from the midpoint of

the stimulating electrode pair. The channel spacing was set to 5 mm by moving the recording electrode pair proximally along the nerve axis for each trace. Data were processed offline using Matlab Version 7.0.4.

C. Velocity Filter

The velocity filter was realized by an FIR approximation using a 2 dimensional window method. An inverse DFT approximation of the ideal discrete frequency response was truncated to a size of 21×51, followed by the application of a 2D window as in [5]. Fig.2 depicts a system diagram of this measurement setup.

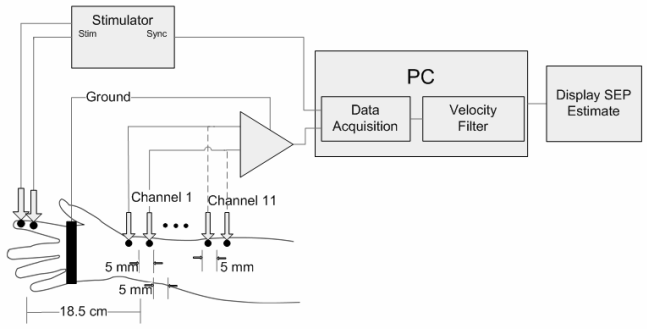

Fig.2 System diagram of SEP measurement setup.

IV. Factors Affecting the Performance

A. Spatial Frequency Resolution

The temporal sampling frequency may be selected to specify the cutoff velocity, choosing a compromise between SEP distortion and SA attenuation [5]. The spatial sampling rate is fixed, however, due to the limited spatial window where the SEP may be observed at the skin surface. In this case, the SEP at the median nerve could be measured from the skin surface within 10 cm along the wrist, starting from the location of the first trace (i.e., 11 channels). The filter performance will therefore be limited by spatial frequency resolution and spectral leakage, which can be viewed as a spatial rectangular window applied to the array:

$$\hat{s}(x,t) = s\left(t - \frac{x}{v}\right)\Pi\left(\frac{x}{\Delta x}\right)$$
$$\hat{S}(k,\omega) = S(\omega)\delta\left(k + \frac{\omega}{v}\right) * \Delta x \operatorname{sinc}\left(\frac{k\Delta x}{2}\right) \quad (8)$$

If the window length (i.e., number of channels) is small, (8) implies significant spectral leakage and loss of frequency resolution in the k dimension. In this work, 11 channels were used with 5 mm spacing spanning a 5.5 cm measurement window. Beyond this it was difficult to obtain consistent SEP information. As a result, some SA energy falls into the passband, and some SEP energy falls in the stopband. Spatial windowing (e.g., Hamming) is not an effective solution because it distorts the trace-to-trace consistency of the SEP. Improving spatial resolution can only be achieved by using more channels if they are available.

B. Physical Array Implementation

Variation in electrode impedance between traces was minimized by collecting one trace at a time using the same electrodes; however, the spatially sampled data are sensitive to the unavoidable human error in position and orientation of the electrodes at each trace. Although extreme care was taken, this source of error will play a role in the filtering performance. In a more practical scenario, a rigid and accurate array structure would be used to collect all channels simultaneously, and pass directly through an A/D converter connected to the velocity filter.

C. FIR Fan Filter Realization

In [5], the authors described an FIR approximation of a fan filter that was used to effectively separate the SA and SEP signals that were generated by simulation models under the assumptions of (4) and (6). As a result of the FIR approximation, the truncated and windowed fan filter suffers from reduced roll-off rate, and passband distortion (more so near the passband edges) as well as poor velocity resolution at low frequencies. To account for this, data must be sampled faster in time such that the $[k,\omega]$ slope in Fig.1 is tilted further into the passband.

D. Trace-to-Trace Consistency

The waveforms containing the SA and SEP at each trace measured as discrete functions of time and axial distance along the nerve axon do not satisfy the assumptions made in (4) and (6) used in the simulations of [5]. The SA experiences a small amount of spreading with axial distance, causing consecutive traces to increasingly lose high frequency content. Since the apparent velocity projected onto the array is the rate of change of temporal-to-spatial frequency, the apparent velocity may not be perfectly resolved. The issue of greater concern, however, is the trace-to-trace consistency of the SEP waveform features. Due to the increase in fiber depth under the skin surface along the nerve axis, the SEP experiences slight spreading as well, with additional attenuation that increases with axial distance (tissue filtering effect). Although the velocity filter produces an accurate estimate of the SEP shape, its amplitude at the center trace is not consistently represented in the measurements. This could result in a scaled estimate and is a topic for further investigation.

V. Results and Discussion

Using the experimental setup described in section III, 11 channels were obtained with a spacing of 5 mm and sampling rate of 50 kHz. This corresponds to a cutoff velocity for the filter of 250 m/sec. By visual inspection, the conduction velocity is approximately 50 to 60 m/sec.

Fig.3 shows every odd numbered channel of the array measurements taken along the median nerve on the wrist, for

better visual representation. Fig.4 shows the region containing the SEP on a smaller scale. By comparing the temporal locations of the negative peaks, the moveout per trace is approximately constant. Slight variations in the moveout may cause some distortion; however, this would be minimized when the measurements are taken with an accurately designed array. It is also observed that the amplitude decreases since the fiber depth increases as a function of axial distance. The effect of this is not analyzed in this paper, but will lead to some distortion in the filter output.

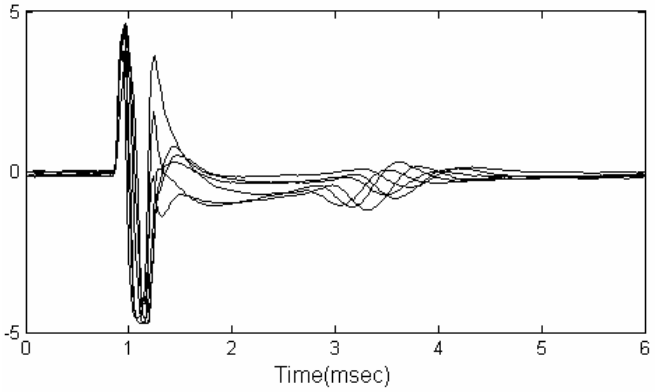

Fig.3 SEP array measurements from median nerve, 6 odd channels from an 11 channel array (1ms pre-trigger duration shown)

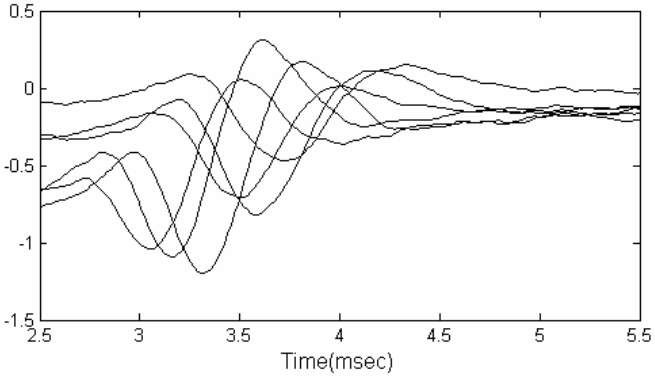

Fig.4 SEP portion of array measurements (6 odd channels from an 11 channel array)

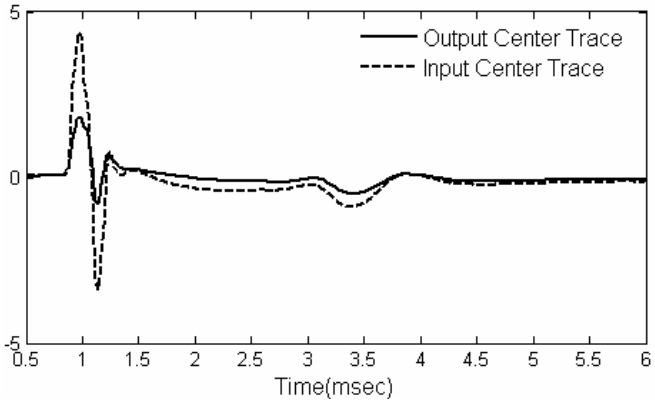

Fig.5 Center traces of the array at the velocity filter input and output.

Fig.5 shows the filter output. The large part of the SA has been severely attenuated, and the slow tail portion has been reduced. The SEP estimate also appears to be slightly distorted even though the conduction velocity is much less than the filter cutoff velocity. This is not due to the filter, but mainly to the increase in fiber depth along the nerve making the SEP appear smaller at the skin surface as a function of axial distance along the nerve. Distortion is also due in part to other factors such as trace-to-trace consistency in moveout and spatial frequency resolution. The distortion however, appears to be a linear scaling factor, preserving the shape from the input trace.

Visually, the output trace in Fig.5 contains less SA interference around the region containing the SEP. One advantage of this is that the latency can be more accurately determined because there is now a better indication of the starting time of the SEP.

VI. Conclusions

In measurement configurations that present temporal overlap of the SA and SEP, using an electrode array with a velocity filter can recover an accurate estimate of the SEP. This has been shown with an 11 channel array measured on the median nerve axis at the wrist with stimulation at the index finger.

When the filter is designed to minimize passband distortion, there may still be additional distortion arising from spatial frequency resolution, trace-to-trace spatial variation of SEP features resulting from electrode impedance mismatches, and trace-to-trace inconsistencies of the SEP observed at the skin surface resulting from physiological effects such as variable fiber depth.

The SA attenuation is large. Therefore, with an array of sensitive, accurately spaced, impedance matched electrodes, the gain in signal-to-noise ratio offered by a velocity filter is large in SEP measurements. The associated cost is that the SEP data be collected at multiple channels to yield a single channel output.

References

[1] V. Parsa, P. A. Parker, "Multireference Adaptive Noise Cancellation Applied to Somatosensory Evoked Potentials," *IEEE Trans Biom Eng*, vol. 41, no. 8, 1994.

[2] R. N. Scott, L. McLean, P. A. Parker, "Stimulus Artifact in Somatosensory Evoked Potential Measurement," *Med Biol Eng Comput*, vol. 35, pp 211-215, 1997.

[3] R. Grieve, B. Hudgins, K. Englehart, "Nonlinear Adaptive Filtering of Stimulus Artifact," *IEEE Trans Biom Eng*, vol. 47, no. 3, 2000.

[4] B. H. Boudreau, K. B. Englehart, A. D. C. Chan, P. A. Parker, "Reduction of Stimulus Artifact in Somatosensory Evoked Potentials: Segmented vs. Subthreshold Training," *IEEE Trans Biom Eng*, vol. 51, no. 7, 2004.

[5] N. Yazdani, A. D. C. Chan, "Stimulus Artifact Reduction in Somatosensory Evoked Potentials by Velocity Filtering," Presented and published in the Proceedings of CMBES-06, Vancouver, B.C. June 1-3, 2006